Journal of Photochemistry and Photobiology A: Chemistry 223 (2011) 71–81

Contents lists available at ScienceDirect

Journal of Photochemistry and Photobiology A: Chemistry

journal homepage: www.elsevier.com/locate/jphotochem

Spectroscopic studies with fluorescein dye—Protonation, aggregation and interaction with nanoparticles

Swati De*, Rikta Kundu

Department of Chemistry, University of Kalyani, Kalyani, Nadia, West Bengal 741 235, India

ARTICLE INFO

Article history:
Received 14 November 2010
Received in revised form 29 May 2011
Accepted 3 July 2011
Available online 22 July 2011

Keywords:
Xanthene dye
Protonation equilibria
Aggregation
Deaggregation
Nanoparticle

ABSTRACT

The interesting protonation reaction between the well-known xanthene dye, fluorescein and Vitamin C (ascorbic acid) has been followed by UV–visible absorption and fluorescence spectroscopy. Ascorbic acid has been observed to exert a profound effect on fluorescein. At high dye concentration, ascorbic acid leads to very efficient deaggregation while at low dye concentration it affects the protonation equilibrium of the dye. In addition to this, stable silver nanoparticles have been incorporated into the above system and interesting results have been noted. While no strong action of the nanoparticles has been observed at low dye concentration, at high dye concentrations, the nanoparticles lead to a more profound effect on the protonation equilibrium of the dye and better deaggregation of dye aggregates. The results are rationalized in terms of the surface effects exerted by the nanoparticles.

1. Introduction

Xanthene dyes are widely studied due to their interesting spectral characteristics and their wide-ranging applications as biological stains, sensitizers, laser dyes, quantum yield standards etc. [1–3]. Two of their important spectral characteristics are their (i) pH–dependent chemical equilibria [4,5] and their (ii) aggregation behavior exhibited at high dye concentration [4,6–9]. Earlier reports indicate significant alteration of the UV–visible absorption and fluorescence spectra both with change of the pH of the medium and with dye concentration [4–9].

In this work, we used fluorescein (FL), a xanthene dye and studied its reaction with a weak reducing agent, ascorbic acid (AA) i.e. vitamin C. Under normal circumstances, we would expect AA to affect only the protonation equilibrium of FL. However, our study reveals interesting effects of AA on the aggregation behavior of the dye also. This unexpected result was investigated in detail. We performed our study in neat water and in micellar media in order to understand the importance of electrostatic and/or hydrophobic interactions on the aggregation process.

Metal nanoparticles are known to often catalyze/retard rates of reactions [10–12]. We also studied the effect of silver nanoparticles on the protonation and/or aggregation behavior of fluorescein in presence of AA. In recent years, there has been an increasing trend towards the study of photophysical and photochemical properties of multicomponent nanostructure assemblies consisting of metals and photoactive dyes. There are few reports which show that association of such dye molecules onto the nanoparticle surface leads to aggregation effects [13,14]. However, to the best of our knowledge, there is no report till date of de-aggregation of xanthene dyes in presence of nanoparticles. Such dye-nanoparticle hybrid species have various applications in optical devices, sensors and in light conversion and imaging [15].

2. Materials and methods

The dye fluorescein (FL) and ascorbic acid (AA) from E-Merck, Germany, was used as such. The surfactants sodium dodecyl sulphate (SDS), cetyl trimethyl ammonium bromide (CTAB) and Triton X-100 (TX-100) were purchased from E-Merck, and were used as such. Concentrated stock solutions (5×10^{-3} M) of dyes were prepared by dissolving weighed amounts in the solvent, the working solutions were then prepared by proper dilution. The final surfactant concentration was fixed at 1×10^{-2} M i.e. much above the respective critical micellar concentration (CMC) of all the three surfactants. The silver nanoparticles were prepared in different surfactant media. The final working [Ag^+] was fixed at 1×10^{-4} M. For all the studies, ascorbic acid was used as the reducing agent.

The absorption spectra were recorded with a Shimadzu UV 2401-PC spectrophotometer (Kyoto, Japan). The fluorescence spectra were recorded with a Perkin Elmer LS 55 spectrofluorimeter. The solutions in this case, were excited both at the maximum of dye absorption and also at the shoulder. In order to excite any species absorbing at shorter wavelengths, we sometimes used

* Corresponding author. Tel.: +91 9831244131; fax: +91 33 25828282.
E-mail address: swati_de1@rediffmail.com (S. De).

1010-6030/$ – see front matter © 2011 Elsevier B.V. All rights reserved.
doi:10.1016/j.jphotochem.2011.07.002

λ_{ex} = 430–435 nm. For recording the excitation spectra, λ_{em} was fixed at 550–570 nm. Fluorescence lifetimes were determined from time-resolved intensity decays by the method of time correlated single photon counting (TCSPC) using a diode (IBH, UK) nanoLED-07 as the light source at 438 nm. The full width at half maxima (FWHM) of this excitation source is 70 ps. The decay curves were analyzed using IBH-6 decay analysis software. The decays were given both single exponential and bi-exponential fits and depending on the χ^2 values and the residuals it was decided to be either single or bi-exponential. The pH of the solutions was measured with a systronics pH-meter. Dynamic light scattering studies were performed with a Nano-ZS (Malvern) instrument, which is equipped with a 4 mW He–Ne laser (λ = 632 nm). The samples for this study were prepared by filtering the solutions with a 0.2 μm filter. The resolution of the experimental setup is 0.6 nm. Transmission Electron Microscopic (TEM) studies of the nanoparticles were carried out at a resolution of 1.9 Å unit with a JEOL, JEM-2100 Electron Microscope from Japan. TEM specimens were prepared by placing micro-drops of solutions on a carbon film supported by a copper grid. The absorption spectra were resolved using the specwin 32 program, based on the principal component analysis (PCA) method [16]. The structures of the different protonated forms of FL have been optimized by MM2 calculations using the software CS Chem. 3D Ultra, Version 10.

3. Results and discussion

It has been previously reported that in aqueous media, FL dye forms aggregates at concentrations greater than 1×10^{-5} M [4,7]. In order to study the effect of AA on dye protonation and aggregation separately, we have performed our study at two different dye concentrations [A] 1×10^{-6} M (non-aggregating concentration) and [B] 1×10^{-4} M (aggregating concentration). Thus the entire work will be discussed for two different dye concentrations.

3.1. Non–aggregating dye concentration, [FL] = 1×10^{-6} M

At [FL] = 1×10^{-6} M, the dye is present in monomeric form only. The absorption spectrum of 1×10^{-6} M FL in neat water (Fig. 1(i)) shows the presence of mainly the dianion with a peak at 485 nm, and a much smaller contribution from the monoanion (shoulder at ~460 nm). Our inference about the different spectral forms of fluorescein dye originates from the work of Margulies et al. [5] and Sjoback et al. [17], where the various protonated forms of fluorescein dye were discussed in detail along with their absorption spectra. (Scheme 1) shows the geometry-optimized structures of the different forms of the dye. Considering the pH of neat water i.e. 6.1 the presence of mainly the dianion along with small amounts of monoanion can be understood, this correlates well with literature [18] (Scheme 2) where the different protonated forms of FL dye and their respective pK_a's are given. As AA was gradually added to the medium, the spectrum undergoes a change i.e. percentage of monoanion increases, and the spectrum resembles the reported monoanion spectrum (with peaks at 475 nm and shoulder at 440 nm) at 5×10^{-5} M AA (Fig. 1(iv)). At this stage, the measured pH of the medium is 4.6. The existence of the monoanion at this stage is understandable from (Scheme 2). It should be noted that the pK_1 of AA is 4.2, thus it is obvious that AA loses a proton at this pH which is taken up by the dye. The monoanion is characterized by a broad spectrum in general [5,17]. As AA is increased, further protonation occurs until the neutral species (characterized by a peak at 435 nm and shoulder at 475 nm) is formed (Fig. 1(v)). At a very high AA concentration i.e. 1×10^{-2} M, when pH of the medium is 3.5, only the neutral dye species exists (Fig. 1 (vi)). Further protonation to the cation i.e. FL^+ does not occur as is obvious from Fig. 1. Thus we observe very good correlation between the appearance of the various protonated forms of FL dye and the respective pK_a values of FL (Scheme 2).

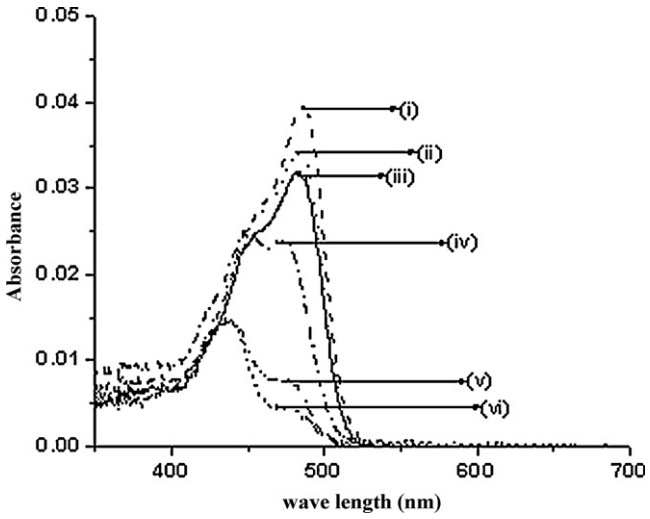

Fig. 1. Absorption spectra of 1×10^{-6} M Fluorescein in neat water, (i) 0 M AA, (ii) 5×10^{-6} M AA, (iii) 1×10^{-5} M AA, (iv) 5×10^{-5} M AA, (v) 1×10^{-3} M AA, (vi) 1×10^{-2} M AA.

Subsequent fluorescence emission studies were undertaken at three excitation wavelengths i.e. 485 nm (to excite the dianion), 460 nm and 435 nm (to excite any lower absorbing species). For λ_{ex} = 485 nm, fluorescence decreases with increase in AA concentration (Fig. 2a). This is because, for FL, the dye dianion and monoanion are usually the more fluorescent species [5,17]. With gradual addition of AA, these species get depleted and are replaced by the weakly fluorescent neutral form of the dye, thus fluorescence decreases. One should keep in mind that at λ_{ex} = 485, we are principally exciting the dianion (λ_{em} = 515 nm). At 460 nm excitation, we are principally exciting the monoanion [5,7,17]. For 460 nm excitation, the fluorescence intensity is much less than for 485 nm excitation but the same trend in fluorescence spectra is observed. However, the fluorescence emission spectra for λ_{ex} = 435 nm differ from those at λ_{ex} = 485 nm and 460 nm. The fluorescence intensity for the former are much less than the latter indicating that, the species absorbing principally at blue wavelengths is not very fluorescent. With increasing AA, fluorescence intensity decreases accompanied by a spectral change – the main dianion emission at 515 nm is seen accompanied by a prominent shoulder at 540 nm. This indicates that the shoulder arises due to emission from some species that absorbs at shorter wavelengths. This may be due to the neutral form of the dye or some dye aggregate. At this stage, it is not possible to assign the exact origin of this new shoulder in the emission spectra. However, at this low dye concentration possibility of existence of dye aggregates is quite low [1,4,6,8,19]. Further, fluorescence excitation spectra were taken keeping λ_{em} fixed at 550 nm. In the fluorescence excitation spectra too, the same trend i.e. the transition dianion → monoanion → neutral is observed as AA increases (Fig. 2b). It may be noted that the fluorescence excitation spectra do not show any splitting thus confirming the absence of aggregates at low dye concentrations [1,4,7,19]. Thus the 540 nm shoulder in the fluorescence emission spectra is not due to dye aggregates.

To comprehend the steady-state fluorescence results well, time-resolved fluorescence studies were carried out. The set-up discussed in Section 2 was used, with λ_{ex} = 438 nm. The results are summarized in (Table 1). The time resolved fluorescence decay of 1×10^{-6} M FL in water fits well to a bi-exponential with time constants of 500 ps and 3.6 ns, the latter being the major component. This is consistent with earlier studies on fluorescein [1,7,17,20].

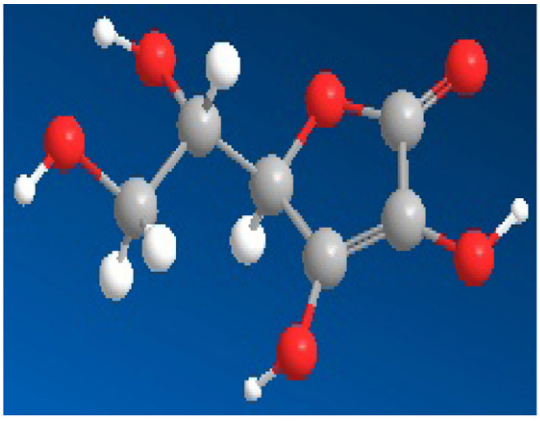

Ascorbic acid

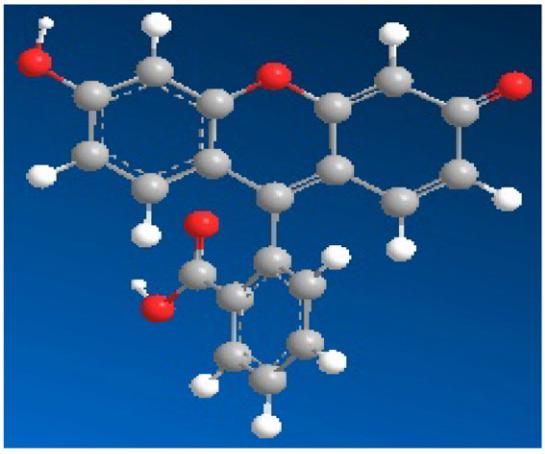

FL Neutral

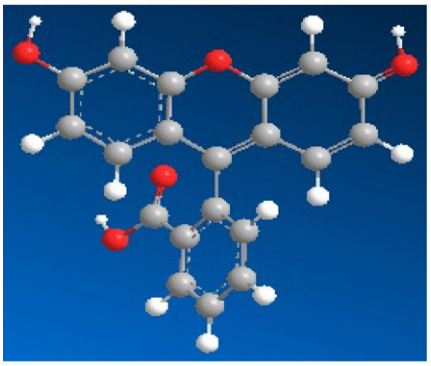

FL cation

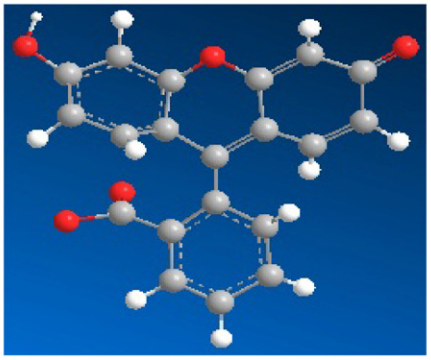

FL monoanion

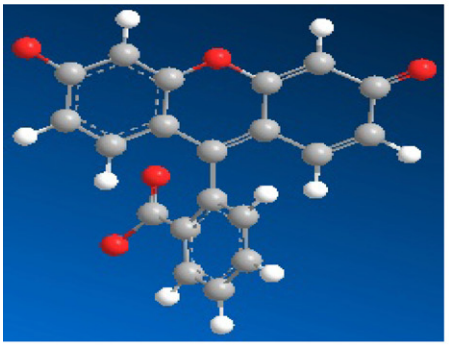

FL Dianion

Scheme 1. Geometry-optimized structures of the various protonated forms of FL dye and ascorbic acid (AA).

Table 1
Time-resolved fluorescence studies of 1×10^{-6} M fluorescein in various media, λ_{ex} = 438 nm.

System	τ_1 (ps)	τ_2 (ps)	a_1	a_2	<τ>(ps)	χ^2
Water						
1×10^{-6} M FL/water	500	3610	0.201	0.7987	2983.8	1.09
1×10^{-6} M FL/water +1×10^{-2} M AA	390	2970	0.1917	0.8082	2475.11	1.04
1×10^{-6} M FL/water + 1×10^{-4} M Ag-np	490	3970	0.317	0.6827	2865.64	1.11
Aqueous TX-100						
1×10^{-6} M FL/1×10^{-2} M TX-100	770	3850	0.2685	0.7314	3022.63	1.04
1×10^{-6} M FL/1×10^{-2} M TX-100 + 1×10^{-4} M Ag-np	500	3810	0.3242	0.6757	2736.51	1.02
Aqueous CTAB						
1×10^{-6} M FL/1×10^{-2} M CTAB	230	4420	0.131	0.8685	3868.9	1.13
1×10^{-6} M FL/1×10^{-2} M CTAB + 1×10^{-2} M AA	720	2475	0.856	0.1437	971.97	1.09
1×10^{-6} M FL/1×10^{-2} M CTAB + 1×10^{-4} M Ag-np	580	4460	0.2233	0.7766	3593.15	1.05
Aqueous SDS						
1×10^{-6} M FL/1×10^{-2} M SDS	825	3930	0.244	0.7559	3171.98	1.06
1×10^{-6} M FL/1×10^{-2} M SDS + 1×10^{-2} M AA	450	3760	0.4096	0.5903	2403.84	1.09
1×10^{-6} M FL/1×10^{-2} M SDS + 1×10^{-4} M Ag-np	720	3990	0.1984	0.8015	3340.83	1.08

τ_1 and τ_2 are the life time components arising out of bi-exponential fits.
a_1 and a_2 are the corresponding amplitudes of these components.
<τ> is the average lifetime given by $a_1\tau_1 + a_2\tau_2$.
χ^2 is the fitting parameter Chi-squared, χ^2 close to 1 means a good fit.

On adding AA to the system, there is slight change i.e. the shorter component is now 390 ps while the larger component is 2.9 ns.

As mentioned earlier, the studies were also performed in micellar media in order to study medium effects on the reaction. All the surfactants were maintained at concentrations much higher than their respective critical micellar concentrations (CMC) to ensure that micelles are formed. First the studies were performed in the neutral surfactant i.e. TX-100, where electrostatic effects are minimized. The spectra indicate that initially in aqueous TX-100, the FL dianion is present. With increasing concentration of AA, the monoanion is generated. However, the neutral species is not formed at all. Thus we note that protonation is much more efficient in neat water compared to aqueous TX-100 as for the latter reaction stops at the monoanion stage and does not proceed to the neutral form.

Next, the cationic micelles formed by CTAB were tried. On adding increasing amounts of AA, the dianion spectrum gets replaced by the monoanion-like spectrum. Here only the monoanion is obtained even at the highest AA concentration i.e. no further protonation to the neutral form is seen. The fluorescence emission spectra of FL show gradual quenching of emission with increase of AA. The distinct difference with water or aqueous TX-100, is that in aqueous CTAB, the additional red shifted emission shoulder at 550 nm is not seen even for shorter λ_{ex} values. This is because the monoanion that is formed participates in electrostatic interaction with cetyl trimethyl ammonium (CTA^+) cation coming from CTAB i.e. the mono-anion has no independent existence. The electrostatic factor also rules out the possibility of aggregation in CTAB at this low dye concentration. Thus the attractive electrostatic interaction

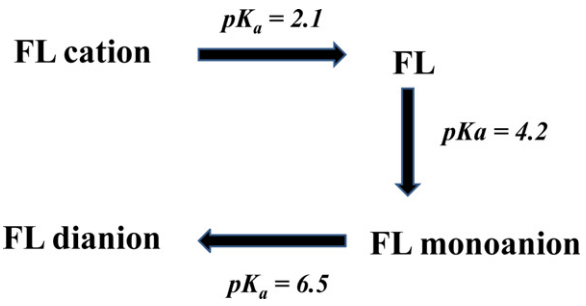

Scheme 2. Scheme showing the protonation equilibria of FL dye along with the respective pK_a's.
(Taken from "*Principles of Fluorescence Spectroscopy*" by J. R. Lakowicz, 2nd ed., Kluwer Academic/Plenum, New York, 1999, Page 638.)

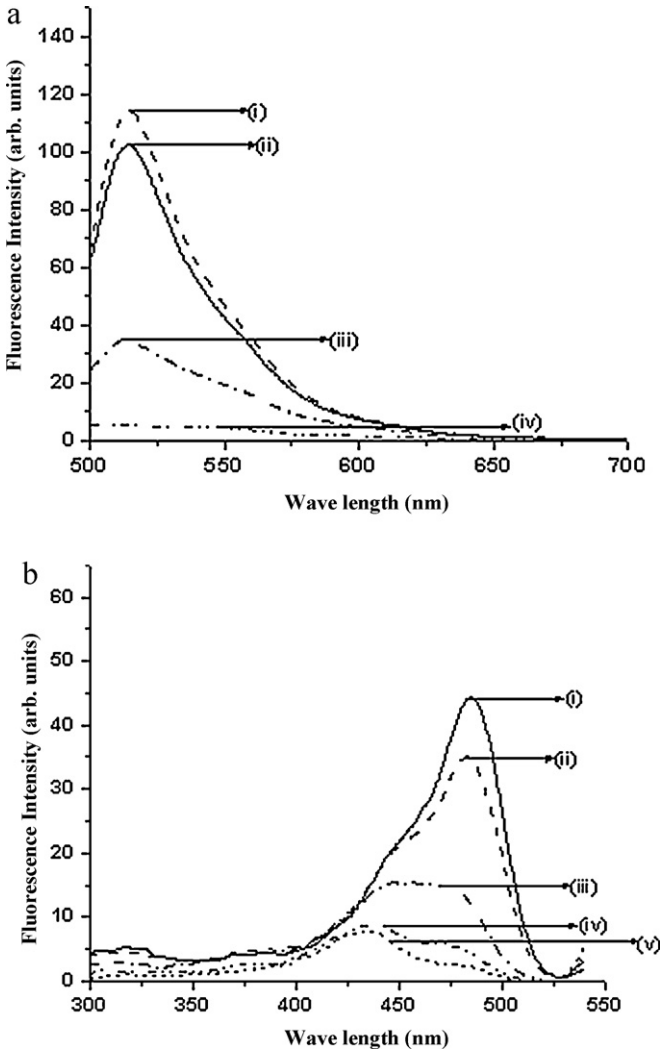

Fig. 2. a. Fluorescence emission spectra of 1×10^{-6} M Fluorescein in neat water (λ_{ex} = 485 nm), (i) 0 M AA, (ii) 1×10^{-5} M AA, (iii) 5×10^{-5} M AA, (iv) 1×10^{-3} M AA. b. Fluorescence excitation spectra of 1×10^{-6} M Fluorescein in neat water (λ_{em} = 550 nm) (i) 0 M AA,(ii) 5×10^{-5} M AA, (iii) 1×10^{-4} M AA, (iv) 1×10^{-3} M AA, (v) 1×10^{-2} M AA.

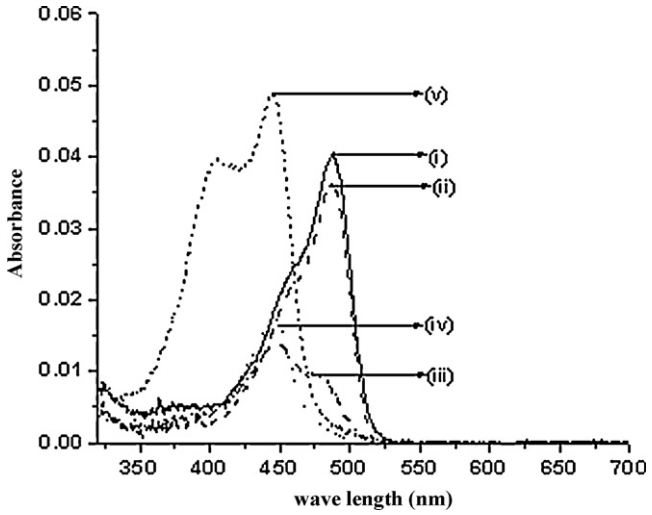

Fig. 3. Absorption spectra of 1×10^{-6} M Fluorescein in aqueous SDS micelles [SDS] = 1×10^{-2} M, (i) 0 M AA, (ii) 1×10^{-5} M AA, (iii) 5×10^{-5} M AA, (iv) 1×10^{-4} M AA, (v) 5×10^{-3} M AA.

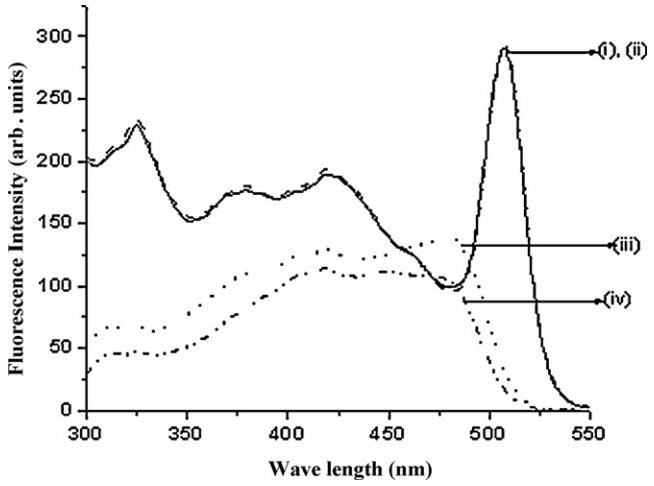

Fig. 4. Excitation spectra of 1×10^{-4} M Fluorescein in neat water (λ_{em} = 570 nm), (i) 0 M AA, (ii) 1×10^{-5} M AA, (iii) 1×10^{-3} M AA, (iv) 1×10^{-2} M AA.

between the negatively charged dye and the positively charged micelle leads to efficient incorporation of the dye by the micelle. In the fluorescence lifetime studies, severe lifetime shortening is observed. This indicates that a fast nonradiative process is depleting the FL excited state in aqueous CTAB micelles. This is because the reaction is faster due to the anchoring effect exerted by CTAB. However, reaction stops at the mono anion stage unlike in water where it proceeds up to the neutral dye form.

Finally, the reaction was performed in an anionic surfactant solution i.e. aqueous SDS micelles. In SDS, the results are unique. Initially up to 1×10^{-5} M AA, the FL dianion-like spectrum is seen. Above this concentration, we almost directly observe the absorption spectrum of the neutral dye i.e. the stage wise transition dianion → monoanion → neutral is not observed [5,17]. Then at higher [AA], the FL cation type spectrum is observed with a peak at 445 nm [5,17]. With further increase in AA concentration, the cation like spectrum along with a new blue shifted peak at 405 nm is seen (Fig. 3). This new peak is most probably a metachromatic peak, due to formation of a ground state complex/aggregate between the newly formed FL cation and SDS anion [21,22]. This metachromatic peak was not observed for the neutral or cationic surfactants, as there the dye cation is not formed. The fluorescence emission results show a sharp drop in fluorescence with increase in AA. This is because the FL cation, which is formed, is non fluorescent. Here too, as for neat water, for shorter excitation wavelength, an additional emission shoulder at 550 nm is observed. It needs to be emphasized here that the red-shifted shoulder in emission is observed only when we see strong indication of formation of the neutral species. The fluorescence excitation spectra indicate the transition from dianion → neutral → cation as AA increases. However, the metachromatic band at 420 nm is not observed, probably because this arises due to ground state complexation and is thus not reflected in excited state fluorescence.

Summarizing the results for low dye concentrations, we find that in neat water protonation of FL dianion by AA proceeds to the neutral stage while for neutral and cationic micelles, protonation stops at the monoanion stage. For the anionic micelle, the protonation proceeds even a step further i.e. to the cation stage and also a new metachromatic band is observed. The fluorescence quenching of FL by AA is due to change in the protonated forms of the dye brought about by AA-induced pH effects. To ascertain the nature of quenching brought about by AA, Stern–Volmer plots were made. However, the Stern–Volmer plots (not shown) are quite nonlinear indicating a complex quenching mechanism [23]. Thus, they are not very informative.

3.2. Aggregating dye concentrations, [FL] = 1×10^{-4} M

The entire study as discussed in the earlier section was also performed at high dye concentrations i.e. 1×10^{-4} M FL where FL is known to form aggregates [1,4,6,7,19]. The absorption spectrum in neat water shows a relatively broad peak centered at ~485 nm with a slight shoulder at ~455 nm. The absorption spectrum for both high and low dye concentration are almost similar except for broadening of the peak for high dye concentrations. This peak broadening is indicative of dye aggregation [1,4,6,7]. With increasing AA, the same transition (dianion → monoanion → neutral) is observed as was seen at low dye concentration. However, here the transition appears to be as follows: dianion aggregate → dianion → monoanion → neutral. Subsequent fluorescence emission studies were undertaken at two excitation wavelengths i.e. 480 nm to excite the dianion and at 455 nm to excite any species absorbing at lower wavelengths. Contrary to the previous section where higher fluorescence emission was observed for λ_{ex} = 485 nm than for lower λ_{ex}, here λ_{ex} = 455 nm gives higher fluorescence intensity than λ_{ex} = 480 nm. This indicates that some species absorbing at shorter wavelengths gives appreciable fluorescence. This is the dianion aggregate which is fluorescent. With increasing AA concentration, emission intensity increases briefly, finally decreasing and is accompanied by a structural change. The increase in fluorescence initially is due to deaggregation caused by AA, whereby the strongly fluorescent dianion monomer replaces the less fluorescent dianion aggregate. The narrow emission spectrum gets replaced by a very broad emission spectrum with a peak centered at 520 nm and a new broad shoulder at 560 nm. The 520 nm peak in fluorescence emission is due to the monomer dianion while the 560 nm shoulder is due to the neutral form/dye aggregates. The fluorescence excitation spectra were taken. The excitation spectrum for the neat dye solution exhibits significant splitting into two sets of bands–one sharp band with a peak at ~515 nm and a relatively broad band with peaks at 420 nm and 375 nm (Fig. 4). Thus, here at high dye concentration, we have strong indication of existence of dye aggregates in solution. Earlier reports [1] have indicated that band splitting implies the existence of both J-type (head–tail) and H-type (head–head) aggregates. The sharp red shifted band at 515 nm is assigned to J-type and the broad blue shifted band to H-type aggregates [4,6,7]. With increasing AA concentration, the split structure is almost lost and finally at the

Table 2
Time-resolved fluorescence studies of 1×10^{-4} M fluorescein in various media, λ_{ex} = 438 nm.

System	τ_1 (ps)	τ_2 (ps)	a_1	a_2	<τ>(ps)	χ^2
Water						
1×10^{-4} M FL/water	980	4270	0.2134	0.7865	3567.48	1.1
1×10^{-4} M FL/water +1×10^{-2} M AA	730	2990	0.276	0.723	2363.25	1.09
1×10^{-4} M FL/water + 1×10^{-4} M Ag-np	730	4570	0.2477	0.7523	3618.83	1.05
Aqueous TX-100						
1×10^{-4} M FL/1×10^{-2} M TX-100	900	4390	0.2325	0.7674	3578.13	1.08
1×10^{-4} M FL/1×10^{-2} M TX-100 + 1×10^{-2} M AA	790	3150	0.4678	0.5321	2045.67	1.11
1×10^{-4} M FL/1×10^{-2} M TX-100 + 1×10^{-4} M Ag-np	960	4380	0.8378	0.1621	1514.28	1.1
Aqueous CTAB						
1×10^{-4} M FL/1×10^{-2} M CTAB	1200	5000	0.2032	0.7967	4227.34	1.12
1×10^{-4} M FL/1×10^{-2} M CTAB +1×10^{-2} M AA	730	2410	0.8598	0.1401	965.29	1.06
1×10^{-4} M FL/1×10^{-2} M CTAB + 1×10^{-4} M Ag-np	690	5130	0.2546	0.7449	3997	1.15
Aqueous SDS						
1×10^{-4} M FL/1×10^{-2} M SDS	850	4410	0.2313	0.768	3583.48	1.07
1×10^{-4} M FL/1×10^{-2} M SDS +1×10^{-2} M AA	700	3540	0.3423	0.6576	2567.51	1.04
1×10^{-4} M FL/1×10^{-2} M SDS + 1×10^{-4} M Ag-np	850	4470	0.2435	0.7564	3588.08	1.07

τ_1 and τ_2 are the life time components arising out of bi-exponential fits.
a_1 and a_2 are the corresponding amplitudes of these components.
<τ> is the average lifetime given by $a_1\tau_1 + a_2\tau_2$.
χ^2 is the fitting parameter Chi-squared, χ^2 close to 1 means a good fit.

highest AA concentration, we have the blue-shifted peak only and a peak at ~475 nm (monomer monoanion) (Fig. 4). Thus, addition of AA to high concentration of FL leads to deaggregation as evidenced from the loss of split structure in the excitation spectrum and also from the absorption spectra. The absorption spectra indicate the formation of the neutral species finally but the excitation spectra do not show this explicitly (Fig. 4). This is because for FL, the dianion and monoanion are the main fluorescent species while the neutral and cationic forms are not fluorescent. Thus, the neutral form, even when existing, does not show up in the fluorescence excitation spectra especially in presence of aggregates. It maybe noted here that at low dye concentration (Section 3.1); the neutral dye spectrum was seen in the excitation spectrum due to the absence of aggregates. The results of the time–resolved emission studies are summarized in (Table 2). The fluorescence decay of 1×10^{-4} M FL in water fits well to a bi-exponential with time constants 0.98 ns and 4.27 ns, the latter being the major component. The lifetime gets shortened indicating a fast depopulation of the fluorescent species with addition of AA.

Studies of the FL-AA system were also carried out in micellar media. First the neutral surfactant, TX-100 was tried. In aqueous TX-100, unlike in water, the absorption spectra are not very broad indicating that dye aggregation is not as efficient here as in neat water. This is because the dye monomers are enveloped by a surfactant jacket, thus monomer–monomer interaction is prevented. Here too, shortening of fluorescence lifetime is observed.

The absorption spectrum of 1×10^{-4} M FL in cationic CTAB micelles, are significantly broad indicating considerable aggregation. With increasing AA, the absorption spectra are gradually converted to that of the monoanionic form, the neutral form is not observed at all, unlike in water. This is because with gradual addition of AA, the pH in neat water is substantially lowered while for micelles the surface pH is not the same as in water [24]. Thus effective pH at the surface of CTAB micelles is not as low as to cause the conversion to the neutral form. It may be recalled here that even for low dye concentration protonation by AA in aqueous CTAB stopped at the monoanion stage. Moreover, FL being an anionic dye participates in favorable electrostatic interaction with the cationic micelle CTAB, thus most of dye is localized at the micellar surface and senses the surface pH on the micelle surface. Thus FL does not sense bulk pH. The fluorescence excitation spectra indicate very distinct splitting into two principal sets of relatively sharp bands, which finally transform to a dianion and then monoanion like spectra. Here both H-type and J-type aggregates are present. For aqueous CTAB micelles, we notice something strange. In the fluorescence excitation spectra, we observe a higher percentage of H-aggregate emission unlike in all other media. Thus our conclusion is that, on addition of AA, these H-aggregates break up to give the monomer dianion and finally the monomer anion. H-aggregate formation in aqueous CTAB is favored due to the electrostatic factor. (Scheme 3) shows how a delicate balance of electrostatic and steric factors may induce preferential H-aggregation at the surface of CTAB micelles. The time resolved studies indicate significant shortening of fluorescence lifetimes with addition of AA, whereby the amplitude values also change i.e. the shorter component becomes the dominating one (Table 2).

Finally the studies were carried out in anionic SDS micelles. It may be recalled that earlier for low dye concentration, the spectra in aqueous SDS micelles were unique where at high AA concentration, the cation-like spectrum was seen along with a new metachromatic band. At high dye concentrations in SDS micelles, the broad absorption spectra typical of dye aggregates are seen. With increasing AA, these are totally transformed to give initially dianion, then monoanion and finally only the cation band at 445 nm, not the metachromatic band. The absence of the metachromatic band for high dye concentrations is because, here the percentage of dye cations is quite large for proportionate complex formation with SDS. Hence, 1:1 complex formation is prevented. Thus the metachromatic signature is not seen. Here too, various λ_{ex} values were tried. Fluorescence intensity was highest for λ_{ex} = 485 nm. The fluorescence excitation spectra show splitting. The time resolved emission studies indicate shortening of lifetimes. Here too, in all the media Stern–Volmer plots (not shown) were tried for the AA-induced fluorescence quenching. Like for low dye concentrations, the plots are quite non-linear indicating complex interaction between AA and FL and hence the plots are inconclusive.

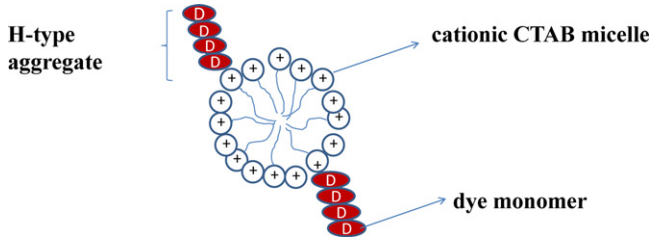

Scheme 3. Preferential H-aggregation of dye molecules at the surface of CTAB micelles.

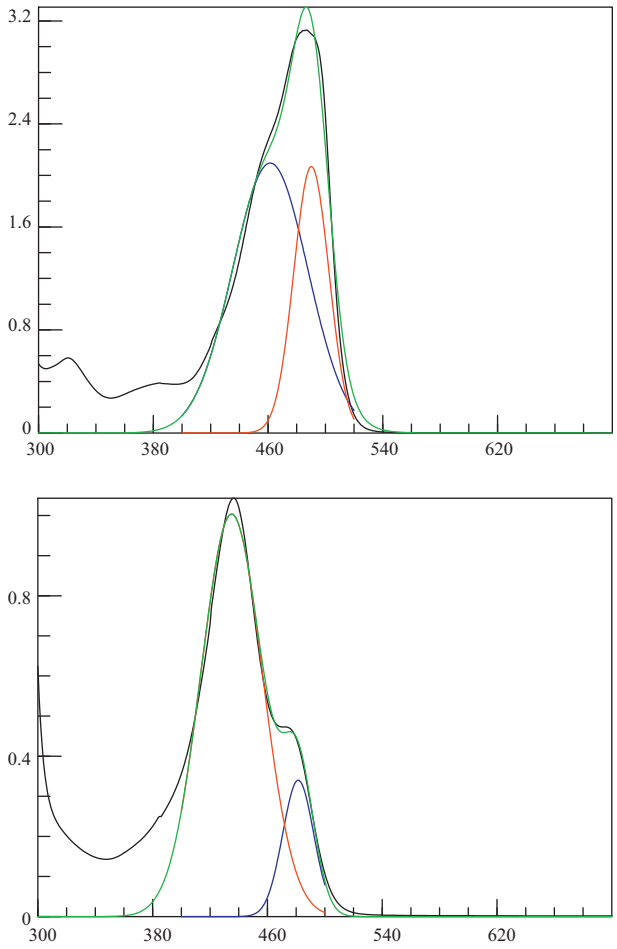

Fig. 5. (a) PCA resolved absorption spectra of 1×10^{-4} M FL in water. (b) PCA resolved absorption spectra of 1×10^{-4} M FL in water + 5×10^{-3} M AA.

The steady-state absorption spectra were resolved using principal component analysis principle (as mentioned in Section 2) [4,16]. For the system 1×10^{-4} M FL in water, the two resolved spectra have components with peaks at 460 nm and 490 nm, respectively with almost equal contributions (Fig. 5a). Thus the absorption spectra of FL at high dye concentrations can be well-resolved into two components. More interesting are the trends observed in the contribution of these two spectral components given by a_1 and a_2. With increasing AA, we see a decrease in a_2 i.e. the contribution of the long component (λ_2). Corresponding, there is an increase in a_1 i.e. contribution of short component (λ_1) (Fig. 5a and b). This justifies our previous discussion about conversion of the FL dianion to the corresponding monoanion or other dye forms absorbing at shorter wavelength. For high dye concentration, the conversion is dianion aggregate → monoanion + some H-type aggregates. While for low dye concentration, the conversion is dianion monomer → monoanion monomer → neutral monomer. Thus the PCA method (whenever it can be applied) is useful to determine the individual spectral components of the composite dye absorption spectrum.

3.3. Effect of silver nanoparticles

Metal nanoparticles have very often been used as model catalysts [10,25–27]. Other workers have also reported dye aggregation, fluorescence quenching [13,14] or enhancement [28] and other interesting effects brought about by nanoparticles. One important point is the stability of the particles synthesized, as the nanoparticles in solution have a tendency to form clusters. Use of suitable capping agent/stabilizers is a viable alternative to form stabilized clusters [28,29]. Thus we have used surfactant-stabilized silver nanoparticles to study their effect on the FL/AA system. We have maintained nanoparticle preparation conditions such that we get a well defined silver plasmon absorption band [11]. The synthesized stable silver nanoparticles were then used for further spectroscopic studies.

Table 3
Result of dynamic light scattering studies of the silver nanoparticles "r_1 and r_2" are the hydrodynamic radii of the particles.

System	r_1 (nm) (a_1)	r_2 (nm) (a_2)	PDI
Ag-np prepared in water	1.73 (0.87)	21.04 (0.13)	1.0
Ag-np prepared in 1×10^{-2} M TX-100	8.72 (0.43)	78.82 (0.57)	0.5
Ag-np prepared in 1×10^{-2} M CTAB	4.2 (0.05)	58.77 (0.95)	0.3
Ag-np prepared in 1×10^{-2} M SDS	3.6 (0.16)	11.7 (0.84)	0.4

r_1 and r_2 are the hydrodynamic radii of the particles.
a_1 and a_2 are the corresponding normalized contributions, PDI is the polydispersity index.

3.3.1. Nanoparticle characteristics

The synthesized nanoparticles were characterized both by dynamic light scattering (DLS) and by transmission electron microscopy (TEM). (Table 3) summarizes the DLS results. The larger radius (r) values in surfactant media correspond to the surfactant – jacketed nanoparticles. Poly dispersity index (PDI) is relatively high in neat water while it is relatively low in surfactant media. Thus, the silver nanoparticles synthesized in surfactant media are reasonably stable and fairly monodisperse. TEM studies show that in neat water, spherical silver nanoparticles with particle diameters in the range of 24–42 nm are formed (Fig. 6a). These cluster together in the absence of any stabilizer [30,31]. In surfactant media, individual spherical nanoparticles are stabilized as is seen from the TEM picture (Fig. 6b). We have used surfactant–stabilized fairly monodisperse silver nanoparticles for our spectroscopic studies.

3.3.2. Interaction of the dye alone with silver nanoparticles (in absence of AA)

In order to study the effect of silver nanoparticles on the FL/AA system, it is first necessary to study the effect of the nanoparticles on the dye alone i.e. without the presence of AA. For this, the dye solution was taken in the four media mentioned in earlier sections (i) neat water (ii) aqueous TX-100 (iii) aqueous CTAB and (iv) aqueous SDS. As usual, studies were performed at low (non-aggregating) and high (aggregating) dye concentrations.

Both at low dye concentration and high dye concentration, addition of increasing concentrations of silver nanoparticles (from a stock silver nanoparticle solution) leads to quenching of the dye fluorescence. Absorption spectra of the dye are not much altered except for increasing predominance of the silver plasmon band at 400 nm. At low dye concentration(1×10^{-6} M FL) maximum fluorescence quenching is observed in aqueous SDS (64%) and neat water media (42%). Since for a constant nanoparticle concentration, the absorption and excitation spectra are not much altered we conclude that the observed quenching is not due to change in structural form of the dye but rather due to the nanoparticles providing an alternative non-radiative decay mechanism [32–34]. Fluorescence quenching is little (10%) for aqueous CTAB medium due to efficient incorporation of the anionic FL dye in the cationic CTAB micelles. The Stern–Volmer plots have been plotted from the steady-state data and are shown in Fig. 7. The Stern–Volmer plots indicate two intersecting straight lines, implying a heterogeneous population of quenchers. Fluorescence lifetimes of the dye in presence of silver nanoparticles have also been determined and are given in Table 1. The lifetimes show slight changes but not much

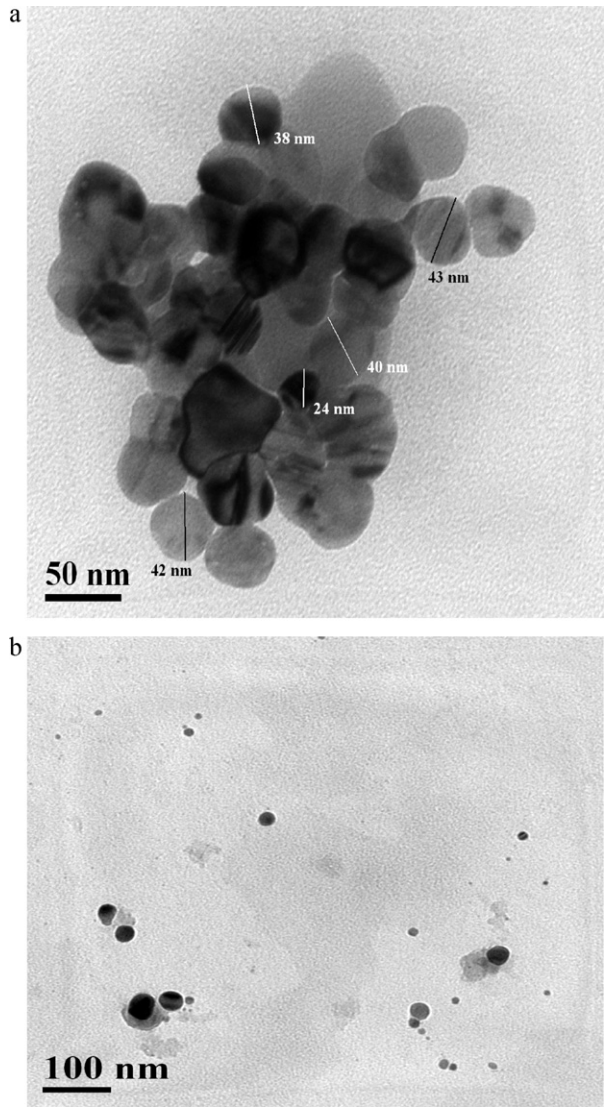

Fig. 6. TEM images of 1×10^{-4} M silver nanoparticles prepared in (a) water (b) SDS micelles.

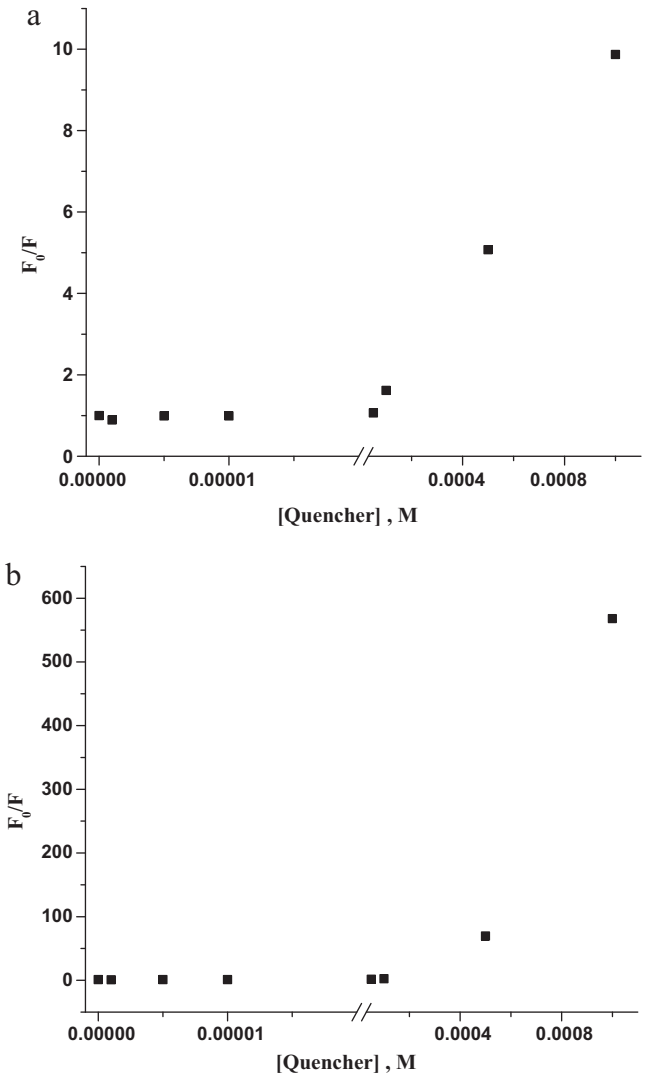

Fig. 7. Stern–Volmer plots for Ag-np induced fluorescence quenching of 1×10^{-6} M FL dye (a) neat water (b) SDS micelles.

difference in presence of nanoparticles indicating that this is a case of static not dynamic quenching. For neutral TX-100 micelles, 30% quenching is observed.

At high dye concentration (1×10^{-4} M), the absorption spectra indicate the existence of dye aggregates. The silver plasmon band at 400 nm is observed for all the media on increasing silver nanoparticle concentration, but is most prominent for aqueous SDS. Concurrently, maximum fluorescence quenching is observed in aqueous SDS media i.e. 85% quenching. For the other media quenching is much less 5% for TX-100, 22% for CTAB and 37% for neat water. For high dye concentrations, the Stern–Volmer plots are quite non linear indicating a complex interaction between the dye and the nanoparticles. To conclude, it can be said quite convincingly that the silver nanoparticles do interact with the dye alone causing considerable fluorescence quenching which is much more than the quenching caused by Ag^+ alone (data not shown). Control experiments were performed to study the quenching effect of Ag^+. It was observed that Ag^+ does not cause any quenching of dye fluorescence except slightly in neat water. Thus the quenching of dye fluorescence by the silver nanoparticles is solely due to the silver nanoparticles and the contribution from Ag^+ ion (remaining unreacted) is negligible.

3.3.3. *Effect of Ag nanoparticles on the protonation/aggregation equilibria of the FL/AA system*

3.3.3.1. At low dye concentration. To study the effect of silver nanoparticles on the process, previously prepared nanoparticles (stock $[Ag^+] = 5 \times 10^{-3}$ M) were added to the aqueous dye solution before addition of AA. The final silver concentration was same in all cases i.e. 1×10^{-4} M. On addition of nanoparticles to the dye solution in neat water, the dye absorbance was completely masked within the wider envelope of the silver plasmon band. Now, with gradual addition of AA the main plasmon band gets widened with the addition of a new hump at ~600 nm. This is indicative of aggregated nanoparticles [30,31] which occurs due to absence of surfactant jacket or arises due to dye–induced perturbations in neat water medium [13,14]. We already have proof of this kind of particle aggregation in neat water from the TEM results (Fig. 6a). Subsequently, fluorescence emission studies were carried out. With increasing AA, fluorescence gets quenched and disappears completely at high AA concentrations. However, the extent of quenching of FL fluorescence on gradual addition of AA is much less in presence of silver nanoparticles than in their absence. One reason for this is that some of the AA is used up for reducing the little amount of free Ag^+ that may still be present and thus complete protonation of dye is not possible. Support for this also comes from the

Table 4
Calculation of the surface-to-volume ratio and number of surface atoms for the various nanoparticles.

System	Diameter(nm) (from TEM study)	α	% Surface atoms
Ag-np in water	24	0.03625	4%
Ag-np in TX-100	19	0.04578	5%
Ag-np in CTAB	15	0.0580	5%
Ag-np in SDS	13	0.06692	7%

N_{Ag} is the aggregation number of the Ag-nanoparticles.
α is their surface-to-volume ratio, N_S is the number of surface atoms.

fluorescence excitation spectra which indicate that finally at very high AA concentrations, reaction stops at the monoanion stage in neat water while in absence of silver nanoparticles, the reaction had proceeded to the neutral dye stage.

The effect of silver nanoparticles on the reaction in aqueous micelles was also studied. In the neutral surfactant TX-100, with increasing AA, new features develop in the nanoparticle spectrum with corresponding color change. For example at 1×10^{-3} M AA, the solution turns orange and double humps are seen at 414 nm and 480 nm. These changes are due to changes in the size/shape of the silver nanoparticles brought about due to interaction with the dye [35]. These observations are consistent with the results of Ghosh et al. and Chandrasekharan et al. [13,14] who observed nanoparticle aggregation for small-sized gold colloids (~10 nm in diameter) brought about by dyes.

In aqueous CTAB micelles, the feature that distinguishes this situation from neat water or aqueous TX-100 is that here the dye absorbance is not totally masked. The dye absorbance appears as a tiny satellite hump at 500 nm even in presence of the strong silver nanoparticle plasmon band. The reason is that FL dianion is strongly anchored to CTAB micelles via the electrostatic effect and thus the dye identity is not completely lost in presence of silver nanoparticle. Indication of such strong anchoring was also mentioned in Section 3.1.

In aqueous SDS micelles, the dye absorption is masked totally by the wider silver nanoparticle plasmon band. With gradual addition of AA, the metachromatic peak develops at ~440 nm even in presence of silver nanoparticles. At higher concentration of AA, the solution becomes orange colored with development of a new hump at 445 nm. This is again due to the change brought about in the shape/size of the nanoparticles by the presence of the dye [13,14]. For SDS, in contrast to other systems, fluorescence emission studies reveal that quenching of FL fluorescence by AA is more efficient in presence of silver nanoparticles than in their absence. However, this can be due to the fact that in SDS micelle, the silver nanoparticles interact strongly with the dye alone even in the absence of AA (Section 3.3.2). We have made some calculations on the surface area and number of surface atoms for the different nanoparticles as suggested by Ghosh et al. [13]. The results are given in (Table 4). We have taken the diameter from the major population of Ag nanoparticles obtained from the TEM studies. For example, for a particle of diameter 24 nm in water, surface-to-volume ratio (α) is 0.03 while for SDS α is ~0.07. Thus the higher α value in SDS micelles may account for the enhanced fluorescence quenching in SDS micelles in presence of nanoparticles. For other media such enhancement in fluorescence quenching is not observed as α values are lower.

As far as the effect of Ag nanoparticles on the protonation reaction is concerned, for all the surfactant systems, except SDS no distinct effect is observed. Rather, incomplete reaction occurs in presence of nanoparticles for neat water, aqueous TX-100 and aqueous CTAB. For aqueous SDS medium, however, there is some effect exerted by the nanoparticles as evidenced by larger fluorescence quenching. On the other hand, the dye exerts some effect

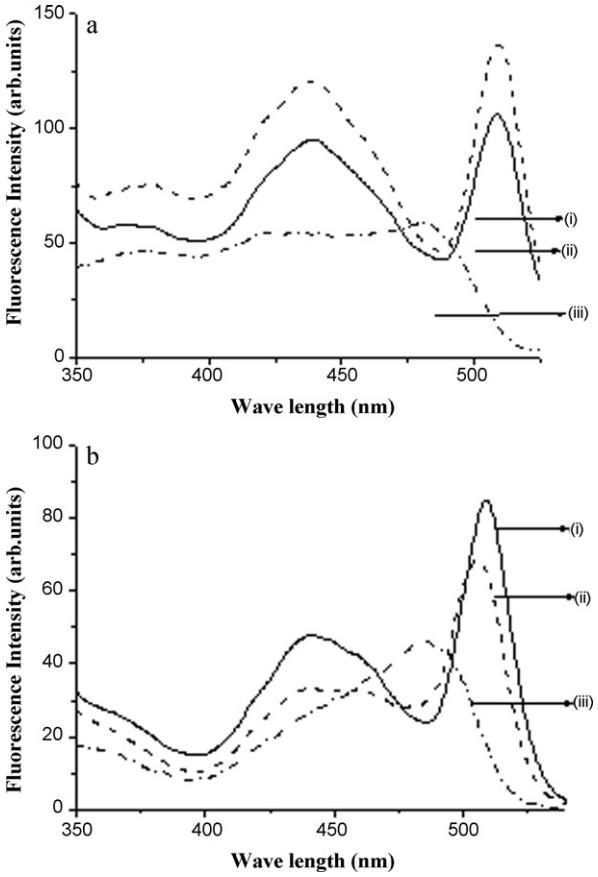

Fig. 8. (a) Fluorescence excitation spectra of 1×10^{-4} M FL in water (in presence of Ag nanoparticles) 0 M AA, (ii) 1×10^{-5} M AA, (iii) 5×10^{-4} M AA. (b) Fluorescence excitation spectra of 1×10^{-4} M FL in aqueous SDS micelles (in presence of Ag nanoparticles) 0 M AA, (ii) 5×10^{-5} M AA, (iii) 5×10^{-4} M AA.

on the size/shape of the nanoparticles for the neutral and anionic surfactants.

3.3.3.2. At high dye concentration. In the earlier section, it was discussed how the presence of silver nanoparticles lead to some alteration in the protonation behavior of the FL/AA system, for low dye concentrations. We also studied the effect of silver nanoparticles at high dye concentrations. Thus the nanoparticles were added to the dye solution prior to the addition of AA. With increasing concentration of AA, there is deaggregation but more AA is required to cause dye de-aggregation, than in absence of nanoparticles. The slower dye deaggregation rate is because part of the AA is used up for reducing some residual Ag^+ ion rather than FL. Finally the transition dianion aggregate → monoanion → neutral is seen even in presence of nanoparticles. The final decrease in fluorescence intensity caused due to protonation is much more in presence of silver nanoparticles. There is a marked difference between the excitation spectra of dye in neat water, with and without nanoparticles. In presence of nanoparticles, J aggregate/H aggregate ratio decreases very fast on adding AA while in absence of nanoparticles, this ratio remains quite high except at really high AA concentration. Thus nanoparticles help to destroy the linear J-aggregates which is an effect that is quite noteworthy (Fig. 8a).

In aqueous CTAB micelles, once again there are differences observed between the protonation behavior in presence and absence of nanoparticles. On subsequent addition of AA, in absence of nanoparticles, deaggregation occurs to give the dianion monomer and finally the monoanion absorption is seen. But in presence of silver nanoparticles, the dianion monomer absorption

spectrum is never seen, deaggregation occurs to give directly the monoanion. This indicates faster deaggregation in presence of silver nanoparticles in aqueous CTAB micelle. The fluorescence excitation spectra indicate that both H and J aggregates are initially present, finally AA causes deaggregation to give first dianion and then monoanion.

In anionic SDS micelles, the same trends in absorption spectra are observed as before. Also, an additional hump at 400 nm, over and above the new metachromatic band at 445 nm is observed in presence of Ag nanoparticles. This is the nanoparticle plasmon peak. Fluorescence excitation spectra indicate loss of splitting in bands i.e. deaggregation. This indicates better deaggregation in presence of Ag nanoparticles (Fig. 8b).

Thus summarizing for high dye concentrations, there is significant effect exerted by silver nanoparticles. In presence of nanoparticles in all the micellar media, we observe better deaggregation compared to the situation without nanoparticles. In neat water, rather than their being enhanced deaggregation in presence of Ag-nanoparticles, we observe very rapid decrease of J-agg/H-agg ratio. Thus, we can categorically state that silver nanoparticles do exert considerable effect on the deaggregation of FL caused by AA i.e. deaggregation is faster in presence of nanoparticles. This finding is quite novel. There are very few reports of such nanoparticles induced dye deaggregation. That dye aggregation may be prevented when dyes adsorb to the surface of gold nanoparticles was shown by Makarova et al. [36] and Templeton et al. [37]. However, many workers have reported the reverse effect i.e. nanoparticle-induced dye aggregation [13,38]. They have shown that small-sized nanoparticles can induce dye aggregation. Our nanoparticles are comparatively larger in size and thus they show the reverse effect i.e. dye de-aggregation. We can explain the accelerated deaggregation of dye aggregates (in presence of nanoparticles) by correlating the structure of the nanoparticles in terms of their surface parameters. The results are summarized in (Table 4). We find that out of the total atoms of Ag for any particle, quite a large number are on the surface. Thus the surface of such a particle can interact with a large number of fluorescein molecules. This leads to strong interaction between the two and thus the nanoparticle-induced quenching and deaggregation effects can be explained.

4. Conclusions

This work reports on the protonation reaction between a common biological probe and a laser dye, FL and vitamin C (ascorbic acid). The effects of silver nanoparticles on the protonation reaction are also explored where principally the dianion monomer exist. At low dye concentrations, we find that the protonation reaction proceeds to the neutral form of FL, in neat water while for aqueous TX-100 and CTAB micelles, the reaction stops at the monoanion stage. For aqueous SDS micelles, reaction proceeds to the cation-stage with subsequent exhibition of metachromasia. Thus as far as aqueous micellar media are concerned, neutral and cationic micelles prevent complete protonation of FL by AA due to shielding/anchoring effects arising out of hydrophobic interactions and electrostatic effects. Also micellar surface pH may play an important role. The anionic micelle SDS displays unique effects. For the anionic micelle, however, repulsive electrostatic interaction forces the anionic dye to remain in the bulk solvent where it is highly susceptible to attack by AA whereby protonation is complete and the dye cation is formed. Subsequently, this dye cation can participate in metachromatic interaction with the anionic surfactant molecules. Thus there is considerable effect exerted by micellar media on the protonation reaction between FL and AA.

At high dye concentrations, the principal species that exist are the dye aggregates: both J-type and H-type. On adding AA to the dye, there is deaggregation due to intermolecular hydrogen bonding between FL and AA. The anionic micelle SDS, too shows interesting effects, here at high dye concentration (unlike for low dye concentration), the metachromatic band is not observed. This is probably due to the existence of excess dye cations preventing stoichiometric complex formation with the surfactant molecules.

Further investigations carried out in presence of silver nanoparticles reveal interesting effects exerted by the nanoparticles. Addition of the nanoparticles to the dye solution in neat water or in aqueous surfactants leads to quenching of the dye fluorescence. Quenching action of nanoparticles is well-known. We have also shown that this quenching is mainly due to the silver nanoparticles and not due to any unreacted Ag^+ ions. Also the dye is found to affect the size/shape of the silver nanoparticles in some cases.

At high dye concentration, presence of silver nanoparticles leads to considerable effects on the aggregation phenomena. For all the four media, nanoparticles accelerate the deaggregation process. Additionally, in neat water, presence of nanoparticles leads to very rapid decrease of the J-aggregate/H-aggregate ratio i.e. nanoparticles disrupt the head-to-tail type dye aggregates, probably due to interception of the intermediate regions between the individual dye monomers.

Thus this work reports on the efficient deaggregation of FL aggregates in presence of weak reducing agents like AA which is promoted by silver nanoparticles. Thus harmless chemicals like AA and/or silver nanoparticles may be efficiently used to prevent aggregation of FL in laser materials, quantum yield standards and in biological labeling. We have not performed exhaustive size-dependent studies with nanoparticles, this may be explored later.

Acknowledgements

S. De thanks DST, New Delhi for generous grant of the SERC Fast Track Scheme No. SR/FT/CS-057/2008. R. Kundu thanks the University of Kalyani for financial assistance in the form of a university research fellowship. We are grateful to Prof. K. Bhattacharyya of IACS, Kolkata for letting us perform the time-resolved fluorescence experiments at the set-up under DST project no. IR/I-1-CF-01/02. We acknowledge Dr. Aparna Datta of IUC-DAE, Salt Lake, Kolkata for letting us use their DLS facility. University of Kalyani is acknowledged for providing the basic infrastructure for research, especially the Shimadzu uv-visible spectrophotometer and Perkin Elmer fluorimeter under the DST-FIST program of the department. We acknowledge CRF, IIT Kharagpur for the TEM studies.

References

[1] M. Kasha, M.A. El-Bayoumi, Energy transfer in hydrogen-bonded N-heterocyclic complexes and their possible role as energy sinks, J. Chem. Phys. 34 (1961) 2181–2186.
[2] Tinoco Jr., Hypochromism in polynucleotides, J. Am. Chem. Soc. 82 (1960) 4785–4790.
[3] B.L. Van Duuren, in: D.M. Hercules (Ed.), Fluorescence and Phosphorescence Analysis, Wiley-Interscience, New York, 1966, pp. 195–215.
[4] S. Das, A.P. Chattopadhyay, S. De Controlling, J aggregation in fluorescein by bile salt hydrogels, J. Photochem. Photobiol. A: Chem. 197 (2008) 402–414.
[5] D. Margulies, G. Melman, A. Shanzer, Fluorescein as a model molecular calculator with reset capabilities, Nat. Mater. 4 (2005) 768–771.
[6] S. De, S. Das, A. Girigoswami, Environmental effects on the aggregation of some xanthene dyes used in lasers, Spectrochim. Acta A 61 (2005) 1821–1833.
[7] S. De, S. Das, A. Girigoswami, Spectroscopic probing of bile salt–albumin interaction, Colloids Surf. B: Biointerfaces 54 (2007) 74–81.
[8] R. Chaudhuri, F. Lopez Arbeloa, I. Lopez Arbeloa, Spectroscopic characterization of the adsorption of rhodamine 3B in hectorite, Langmuir 16 (2000) 1285–1291.
[9] H.V. Berlepsch, S. Kirstein, R. Hania, C. Didraga, A. Pugzlys, C. Bottcher, Stabilization of individual tubular *J*-aggregates by poly(vinyl alcohol), J. Phys. Chem. 107B (2003) 14176–14184.
[10] N.R. Jana, T.K. Sau, T. Pal, Growing small silver particle as protonation catalyst, J. Phys. Chem. B 103 (1999) 115–121.

[11] A. Henglein, Physicochemical properties of small metal particles in solution: microelectrode reactions, chemisorption, composite metal particles, and the atom-to-metal transition, J. Phys. Chem. 97 (1993) 5457–5471.
[12] A. Henglein, Small-particle research: physicochemical properties of extremely small colloidal metal and semiconductor particles, Chem. Rev. 89 (1989) 1861–1873.
[13] S.K. Ghosh, A. Pal, S. Nath, S. Kundu, S. Panigrahi, T. Pal, Dimerization of eosin on nanostructured gold surfaces: size regime dependence of the small metallic particles, Chem. Phys. Lett. 412 (2005) 5–11.
[14] N. Chandrasekharan, P.V. Kamat, J.Q. Hu, G. Jones, Dye-capped gold nanoclusters: photo induced morphological changes in gold/rhodamine 6G nanoassemblies, J. Phys. Chem. 104B (2000) 11103–11109.
[15] P. Xu, H. Yanagi, Fluorescence patterning in dye-doped sol–gel films by generation of gold nanoparticles, Chem. Mater. 11 (1999) 2626–2628.
[16] Y.P. Sun, D.F. Sears Jr., J. Saltiel, F.B. Mallory, C.W. Mallory, C.A. Buser, Principal component-three component self-modeling analysis applied to *trans*-1,2-di(2-naphthy1)ethane fluorescence, J. Am. Chem. Soc. 110 (1988) 6974–6984.
[17] R. Sjoback, J. Nygren, M. Kubista, Absorption and fluorescence properties of fluorescein, Spectrochim. Acta 51A (1995) L7–L21.
[18] J.R. Lakowicz, Principles of Fluorescence Spectroscopy, 2nd ed., Kluwer Academic/Plenum, New York, 1999, 638.
[19] J.E. Selwyn, J.I. Steinfield, Aggregation equilibria of xanthene dyes, J. Phys. Chem. 76 (1972) 762–774.
[20] E. Rousseau, M.M. Koetse, M. Vander Auweraer, F.C. De Schryver, Comparison between J-aggregates in a self-assembled multilayer and polymer-bound J-aggregates in solution: a steady-state and time-resolved spectroscopic study, Photochem. Photobiol. Sci. 1 (2002) 395–406.
[21] A.K. Mandal, M.K. Pal, Spectral analysis of complexes of the dye, 3,3′-diethyl thiacyanine and the anionic surfactant, SDS by the principal component analysis method, Spectrochim. Acta 55A (1999) 1347–1358.
[22] A. Goswami, M.K. Pal, Spectroscopic probes of the interactions of the dye stains-all with deoxycholate and cholate, Colloids Surf. 10B (1998) 149–159.
[23] J.R. Lakowicz, Principles of Fluorescence Spectroscopy, 2nd ed., Kluwer Academic/Plenum, New York, 1999.
[24] P. Mukherjee, K. Banerjee, A study of the surface pH of micelles using solubilized indicator dyes, J. Phys. Chem. 68 (1964) 3567–3574.
[25] G. Schmid, Large clusters and colloids. Metals in the embryonic state. G. Schmid, Chem. Rev. 92 (1992) 1709–1727.
[26] L.N. Lewis, Chemical catalysis by colloids and clusters, Chem. Rev. 93 (1993) 2693–2730.
[27] D.S. Miller, A.J. Bard, G. McLendon, J. Ferguson, Catalytic water reduction at colloidal metal "Microelectrodes". Theory and experiment, J. Am. Chem. Soc. 103 (1981) 5336–5341.
[28] A.M. Junior, H.P.M. Oliveira, M.H. Gehlen, Preparation of silver nanoprisms using poly (*N*-vinyl-2-pyrrolidone) as a colloid-stabilizing agent and the effect of silver nanoparticles on the photophysical properties of cationic dyes, Photochem. Photobiol. Sci. 2 (2003) 921–925.
[29] J.H. Fendler, Atomic and molecular clusters in membrane mimetic chemistry, Chem. Rev. 87 (1987) 877–899.
[30] A. Henglein, Colloidal silver nanoparticles: photochemical preparation and interaction with O_2, CCl_4, and some metal ions, Chem. Mater. 10 (1998) 444–450.
[31] F. Chen, R.L. Johnston, Plasmonic properties of silver nanoparticles on two substrates, Plasmonics 4 (2009) 147–152.
[32] P.V. Kamat, Photophysical, photochemical and photocatalytic aspects of metal nanoparticles, J. Phys. Chem. 106B (2002) 7729–7744.
[33] L. Zang, C.Y. Liu, X.M. Rem, Colloidal silver as a quencher for the fluorescence of 2-naphthalenesulfonic acid, J. Chem. Soc. Chem. Commun. 4 (1995) 447–448.
[34] S. De, A. Pal, N.R. Jana, T. Pal, Anion effect in linear silver nanoparticle aggregation as evidenced by efficient fluorescence quenching and SERS enhancement, J. Photochem. Photobiol. 131A (2000) 111–123.
[35] K. Belser, T.V. Slenters, C.P. Fumbidzai, G. Upert, L. Mirolo, K.M. Fromm, H. Wennamers, Silver nanoparticle formation in different sizes induced by peptides identified within split-and-mix libraries, Angew. Chem. Int. Ed. 48 (2009) 3661–3664.
[36] O.V. Makarova, A.E. Ostafin, H. Miyoshi, J.R. Norris, D. Miesel, Adsorption and encapsulation of fluorescent probes in nanoparticles, J. Phys. Chem. 103B (1999) 9080–9084.
[37] A.C. Templeton, W.P. Wuelfing, P.W. Murray, Monolayer-protected cluster molecules, Acc. Chem. Res. 33 (2000) 27–36.
[38] N. Kometani, M. Tsubonishi, T. Fujita, K. Asami, Y. Yonezawa, Preparation and optical absorption spectra of dye-coated Au, Ag, and Au/Ag colloidal nanoparticles in aqueous solutions and in alternate assemblies, Langmuir 17 (2001) 578–580.